Raman scattering and photoluminescence in Cu_2O under hydrostatic pressure

K. Reimann and K. Syassen
Max-Planck-Institut für Festkörperforschung, Heisenbergstrasse 1, D-7000 Stuttgart 80, Federal Republic of Germany
(Received 18 January 1989)

Excitonic transitions and phonon frequencies in Cu_2O were measured by luminescence and Raman spectroscopy at hydrostatic pressures up to 8.5 GPa and at a temperature of 6 K. The exciton Rydberg energy is found to decrease at a rate of -2.4 meV/GPa. The band gap increases at a rate of 12.5 meV/GPa, which corresponds to a band-gap deformation potential of -1.38 eV. The electron-hole exchange energy, i.e., the energy difference between orthoexciton and paraexciton, is independent of pressure. The mode Grüneisen parameters for the zone-center phonons vary between -3.4 and $+1.7$. A rigid-ion model for the pressure dependence of $\mathbf{k}=\mathbf{0}$ phonon frequencies yields mode Grüneisen parameters which are consistent with the experimental data.

I. INTRODUCTION

Cuprous oxide (Cu_2O) is a prototype material for the study of excitonic transitions in semiconductors. Since the discovery of excitons in Cu_2O (Ref. 1), a large amount of work has been reported on the optical and vibrational properties of Cu_2O (see, e.g., Refs. 2–5). Whereas the high-pressure behavior of the tetrahedrally coordinated zinc-blende and wurtzite family of semiconductors has been studied extensively, the behavior of excitons and phonons in Cu_2O under hydrostatic pressure is largely unexplored. To our knowledge the only work on this field was reported by Kreingol'd *et al.*[6] and by Laisaar *et al.*,[7] who investigated the pressure dependence of exciton energies at a temperature of 77 K at moderate pressures up to 0.1 and 1.2 GPa, respectively. In this paper we present results of a low-temperature investigation of excitons and phonons in Cu_2O at hydrostatic pressures up to 8.5 GPa, thus covering almost the full stability range of the ambient pressure phase.[8]

The properties of Cu_2O, which are relevant to the present paper, are briefly summarized as follows. Cu_2O crystallizes in the cuprite structure, which belongs to the space group O_h^4 or $Pn3m$ (point symmetry O_h or $m3m$), i.e., it has inversion symmetry. The unit cell contains two molecules. Thus there exist 15 zone-center optical phonons. The symmetry classification of the optical phonons is[9,10]

$$\Gamma_2^- + \Gamma_3^- + 2\Gamma_4^- + \Gamma_5^+ + \Gamma_5^- \ .$$

Using group theory one finds the normal modes of these phonons[11,12] labeled A to F (see also Fig. 1): A (Γ_5^-) rotation of the Cu tetrahedron about its center; B (Γ_3^-) same motion as A, but the upper two atoms move out of phase with the lower two; C (Γ_4^-) out-of-phase beating motion of two Cu pairs [e.g., in the (110) and ($1\bar{1}0$) planes, in-plane beating]; D (Γ_2^-) breathing mode of the Cu tetrahedron; E (Γ_5^+) shearing motion of the O planes; and F (Γ_4^-) beating of the Cu and O sublattices. Because the phonons C and F both have the same symmetry, some mixing between them will occur. Further, these phonons are infrared active, which results in their splitting into transverse (C',F') and longitudinal (C,F) phonons.

Cu_2O is a direct-gap semiconductor with a band gap[13] of 2.1720 eV at 2 K. The lowest conduction band has Γ_6^+ symmetry; the highest valence band, Γ_7^+ symmetry.[9] Electrons and holes from these bands form the so-called yellow exciton series. Other exciton series of Cu_2O (i.e., the green, the blue, and the indigo one) are not considered in this work. Since both the lowest conduction band and the uppermost valence band have even parity, S exciton transitions of the yellow series are dipole forbidden. They are allowed, e.g., in quadrupole absorption,[14] two-photon absorption,[4] or with the participation of an odd-parity phonon, as seen in the shape of the absorption edge,[15] in phonon-assisted luminescence,[16] or in resonant Raman scattering.[13] Both valence and conduction band are twofold degenerate because of spin. This results in a fourfold degeneracy of the $1S$ exciton, which is partially lifted by exchange interaction to form a threefold degen-

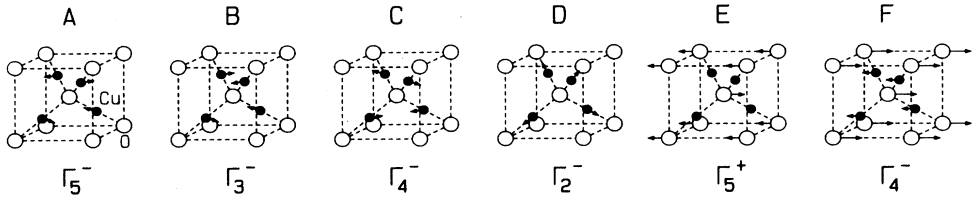

FIG. 1. Schematic representation of zone-center phonon modes in Cu_2O.

 ©1989 The American Physical Society

erate orthoexciton with total spin $S=0$ and a single paraexciton with $S=1$. P excitons of the yellow series are dipole allowed; they form a perfect hydrogenlike series, which was measured up to the principal quantum number[17] $n=9$.

High-pressure Raman and luminescence measurements of Cu_2O were performed at a temperature of 6 K, where nearly perfect hydrostatic conditions were ensured by using condensed helium as a pressure medium. The information on the pressure dependence of zone-center mode frequencies from Raman scattering is supplemented by the observation of phonon sidebands in exciton luminescence. Furthermore, from luminescence measurements we obtain the pressure dependence of the yellow exciton series, i.e., the $1S$ exciton Rydberg energy, the band-gap energy, and the $1S$ electron-hole exchange energy. A simple rigid-ion model is used to calculate the pressure dependence of the phonon frequencies and to determine the amount of mixing between the C and F modes (see Fig. 1).

The remainder of this paper starts with a brief description of the experimental setup. In Sec. III the results of luminescence and Raman measurements are presented and discussed. Finally, we discuss a rigid-ion model for the phonon frequencies in Cu_2O and their pressure dependence.

II. EXPERIMENT

The Cu_2O samples were single crystals thinned down to about 20 μm thickness and cleaved to about 100 μm edge length. For pressure experiments we have used a gasketed diamond-anvil cell (DAC) which is similar in design to that described in Ref. 18, but smaller in dimension. The exciton lines of Cu_2O are extremely sensitive to nonhydrostatic stress components. Therefore, helium was used as pressure medium. For loading, the cell was immersed into superfluid helium.

For optical measurements, the pressure cell was placed in a flow cryostat and cooled down to a temperature of 6 K. The actual temperature of the sample was slightly higher (8 K) due to laser heating, as inferred from the line shape of the phonon-assisted luminescence peaks. The pressure was determined by the ruby luminescence method,[19] using the pressure scale of Mao *et al.*[20] with a zero pressure value for the R_1 line at 6 K of 693.39 nm. In order to minimize uniaxial stress components, which would result in a splitting of the exciton lines, pressure changes were always made at room temperature. Details of the high-pressure and cryogenic experimental setup as well as an investigation of the amount of uniaxial stress sustained in a helium pressure medium at low temperatures will be presented elsewhere.[21] Here, we only note that from the linewidth of the exciton luminescence in Cu_2O we estimate the maximum uniaxial stress to be less than 0.01 GPa at 5 GPa.

The optical setup for luminescence and Raman measurements consisted of an $f/1.4$ collection optics, a 0.5-m double spectrometer, a cooled GaAs photomultiplier, and photon-counting electronics. The 514.5-nm line of an argon-ion laser was used for excitation at power levels of about 100 mW. This excitation energy is above the band gap of Cu_2O at all pressures studied here.

III. EXPERIMENTAL RESULTS AND DISCUSSION

Experimental spectra obtained for different pressures under 2.409 eV laser excitation are shown in Figs. 2–4. The spectrum of the emitted radiation consists mainly of three contributions.[22]

(i) The stokes-shifted Raman spectrum close to the laser energy (Fig. 2).

(ii) The luminescence from the P excitons at about 2.15 eV (Fig. 3).

(iii) The $1S$ orthoexciton luminescence at about 2.05 eV, its phonon sidebands, and the phonon-assisted paraexciton luminescence (Fig. 4).

We will consider the pressure dependence of phonons and excitons separately.

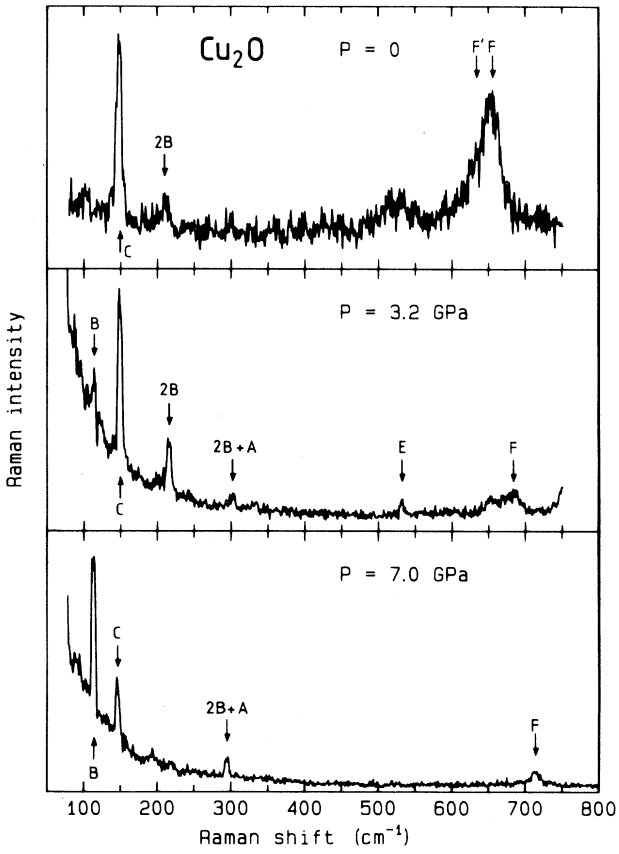

FIG. 2. Raman spectra of Cu_2O for different pressures. The letters denote the phonons involved according to the labeling in Fig. 1.

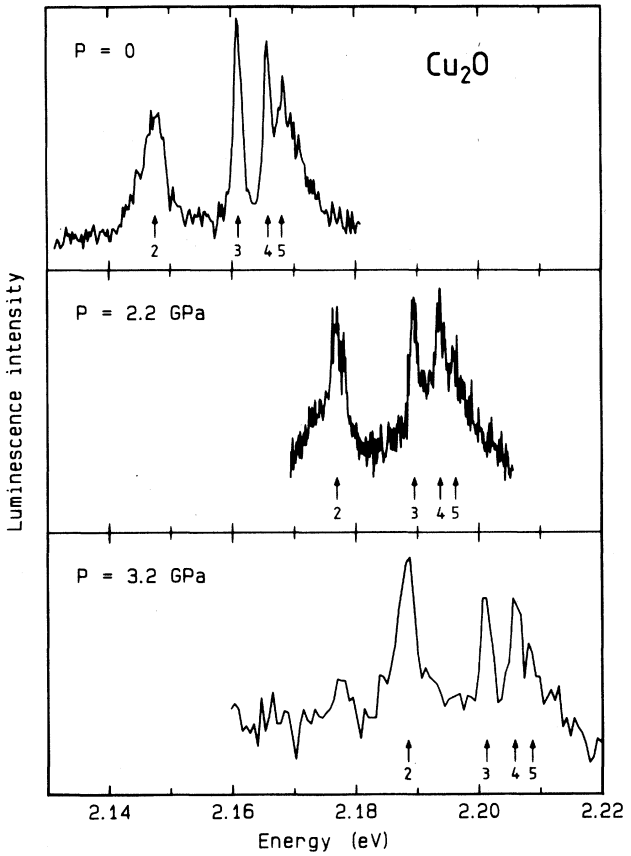

FIG. 3. Luminescence spectra of the P excitons in Cu_2O at different pressures ($T=6$ K). The peaks are labeled with their corresponding main quantum number.

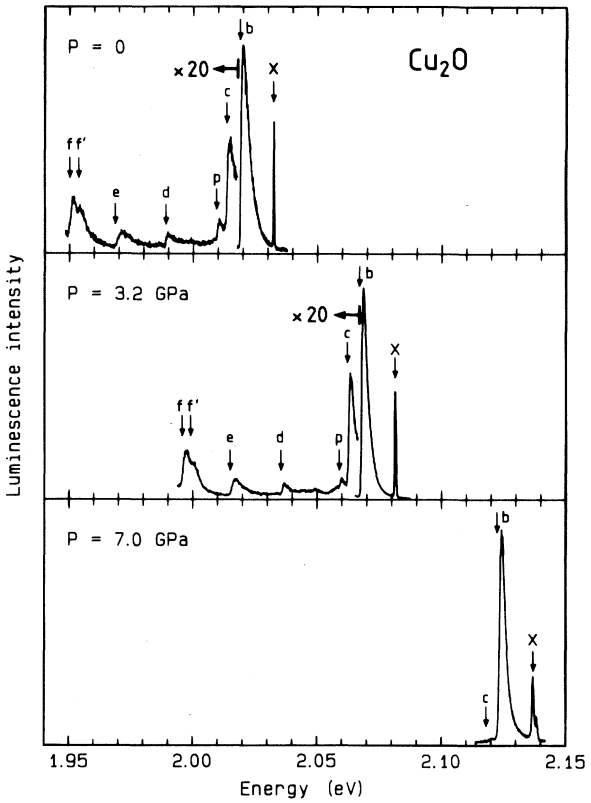

FIG. 4. Luminescence spectra of the $1S$ exciton and its phonon sidebands in Cu_2O. X is the free $1S$ orthoexciton luminescence, $b, \ldots, f'$ are phonon sidebands of the orthoexciton with the participation of phonons $B, \ldots, F'$, and p is the phonon sideband of the $1S$ paraexciton with phonon A.

A. Phonon energies under pressure

It was possible to obtain Raman spectra for pressures up to 8.5 GPa. This limitation is imposed by the pressure-induced phase transition[8] of Cu_2O near 10 GPa. To achieve a pressure of more than 8.5 GPa at 6 K one would have to start at room temperature with a pressure above the phase transition pressure of 10 GPa, because, in our experimental setup, the pressure drops by about 1.5 GPa upon cooling from 300 to 6 K. The hexagonal high-pressure phase showed no Raman signal at all, so Cu_2O in this phase is possibly metallic.

Both the Raman spectra and the luminescence spectra show more phonon bands than one would expect from group theory. So of all zone-center phonons only phonon E is Raman allowed, but one can see, e.g., also the phonons B and C in the Raman spectra (Fig. 2). On the other hand, phonon E also shows up in luminescence (Fig. 4), where it is forbidden. This breakdown of the selection rules in the case of Cu_2O is long known[16,22] and is ascribed to defects, nonstoichiometry, and to the resonant excitation.

The exact values for the phonon energies $\hbar\Omega$ are found from a fit to the experimental spectra. In the case of the Raman lines a Gaussian line shape is assumed. The phonon sidebands in luminescence have a shape of the form[22,23]

$$I(E) \propto \sqrt{\Delta E}\, \exp(-\Delta E/k_B T_x)\ , \quad \text{with} \quad \Delta E = E-(E_x-\hbar\Omega)\ , \tag{1}$$

where E_x is the exciton energy and T_x the excitonic temperature. In Eq. (1) the square-root term stems from the exciton density of states, and the exponential factor gives the thermal occupation within the exciton band. In this form Eq. (1) is valid when the energy bands are parabolic, the exciton system is in thermal equilibrium, and the exciton density is low enough that Maxwell-Boltzmann statistics can be used. Under our experimental conditions all these requirements are met, which results in an excellent fit of the spectra by Eq. (1). As already mentioned, in the present experiments the temperature T_x is slightly higher than the temperature of the cell (8 versus 6 K).

Since phonon A is neither seen in one-phonon Raman scattering nor as a phonon sideband of the $1S$ orthoexciton, its energy was calculated using the three-phonon Ra-

man peak $2B + A$. The sideband of the $1S$ paraexciton (p in Fig. 4) cannot be used, since the free paraexciton luminescence is not seen. This luminescence is only allowed under nonisotropic stress.[24] The fact that it is not seen in our spectra demonstrates the nearly perfect hydrostatic conditions.

All measured phonon energies as a function of pressure are shown in Fig. 5. The values from Raman scattering and from luminescence agree very well except for phonon F. The small differences there arise probably because the peak seen in Raman scattering is not only due to the longitudinal phonon (F) but to some extent also to the transverse phonon (F'). For the phonon C the longitudinal-transverse splitting is too small to be observed. The dashed lines in Fig. 5 represent results of fits assuming a linear pressure dependence. For the fit, the values at zero pressure were taken from the work of Petroff *et al.*[16] The pressure derivatives of the phonon energies and the mode Grüneisen parameters are listed in Table I. The Grüneisen parameter γ is defined as

$$\gamma = -\frac{d\ln(\Omega)}{d\ln(V)} = \frac{B}{\Omega(0)}\frac{d\Omega}{dP} . \quad (2)$$

For the bulk modulus B we have used a value of $B = 110.6$ GPa (Ref. 25).

Neither the phonon frequencies nor the exciton energies show any indication for a phase transition at 5 GPa, which was claimed by Kalliomäki *et al.*[26] As already stated by Werner and Hochheimer,[8] probably large uniaxial stresses were present in the experiment by Kalliomäki *et al.*, which could result in partial decomposition of the sample and a change of phase transition pressures.

One should note the difference in the Grüneisen parameter between the low-energy phonons (A,B,C) on the one hand and the high-energy phonons (D,E,F,F') on the other hand. Whereas the second group shows "normal" values between 1.1 and 1.7, the values for the first group are rather small or even negative. In Sec. V a lattice dynamical model is presented which accounts for the different pressure dependences of the frequencies of these two groups of phonons.

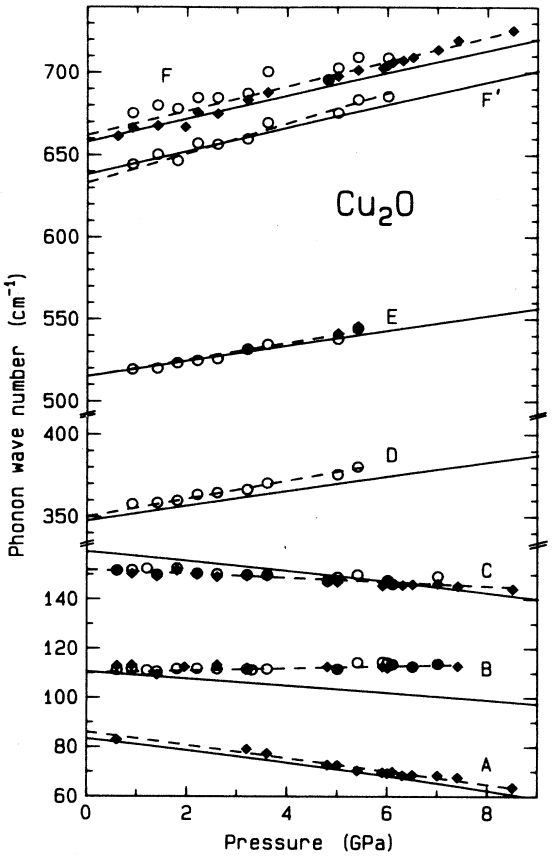

FIG. 5. Pressure dependence of the phonon energies in Cu_2O. The experimental values from Raman scattering are marked by solid diamonds, the values from luminescence by open circles. The dashed lines correspond to the results of fitting a linear relation to the experimental data. The solid lines are calculated from the rigid-ion model (see text).

B. Exciton energies under pressure

The $1S$ exciton could be followed up to 7.0 GPa and the P excitons up to 3.2 GPa. In these cases the limitation was due to increasing background luminescence of unknown origin. Because the luminescence intensity from the P excitons is about two orders of magnitude weaker than the $1S$ exciton luminescence, the corresponding pressure limit is much lower.

The exciton energies as a function of pressure are shown in Fig. 6. For the $1S$ orthoexciton and for the

TABLE I. Phonon frequencies at ambient pressure (Ref. 16), their linear pressure coefficients, and the corresponding mode Grüneisen parameters γ. For convenience, the symmetry classification is given in three notations. The uncertainty for the pressure coefficients is ± 0.2 cm^{-1}/GPa.

Phonon	Symmetry	$\tilde{\nu}_0$ (cm^{-1})	$d\tilde{\nu}/dP$ (cm^{-1}/GPa)	γ
A	Γ_5^- Γ_{25} T_{2u}	86	−2.7	−3.4
B	Γ_3^- Γ_1' E_u	110	+0.4	+0.4
C	Γ_4^- Γ_{15} T_{1u}	152	−0.8	−0.6
D	Γ_2^- Γ_2' A_{2u}	350	+5.5	+1.7
E	Γ_5^+ Γ_{25} T_{2g}	515	+5.1	+1.1
F'	Γ_4^- Γ_{15} T_{1u} TO	633	+9.1	+1.6
F	Γ_4^- Γ_{15} T_{1u} LO	662	+7.4	+1.2

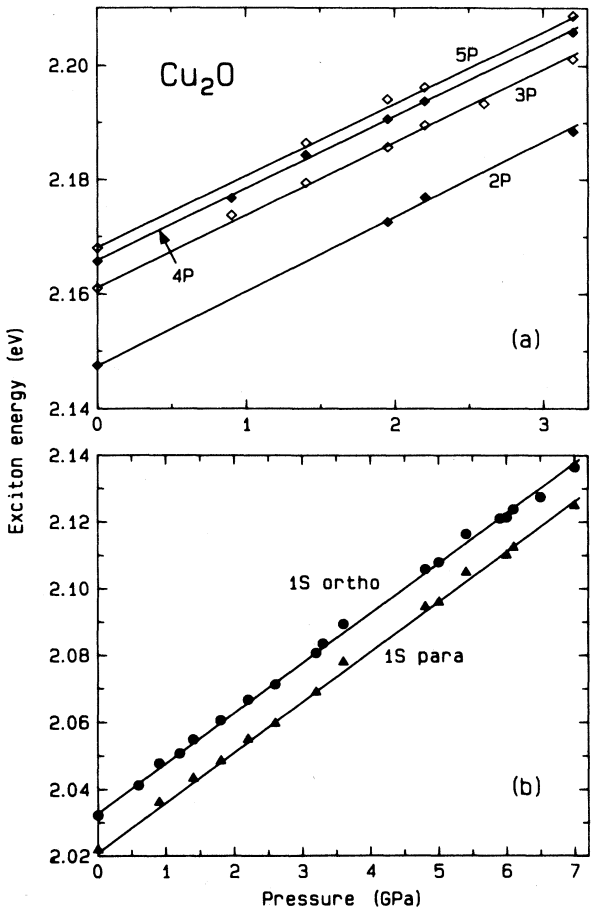

FIG. 6. Exciton energies in Cu_2O as a function of pressure. The solid lines follow from a fit of the pressure dependence of the band gap and the exciton Rydberg.

$2P, \ldots, 5P$ excitons the energy can be taken directly from the luminescence spectra (peak X in Fig. 4 and peaks 2, . . . , 5 in Fig. 3, respectively). The energy of the $1S$ paraexciton was found from its phonon sideband (p in Fig. 4) by adding the energy of phonon A as determined above.

At ambient pressure the P excitons in Cu_2O are the textbook example for a hydrogenlike exciton series, i.e., their energies are given by $E(n)=E_g-n^{-2}R$, n being the principal quantum number, $E_g=2.1720$ eV the band-gap energy, and $R=98.5$ meV the exciton Rydberg. We have assumed that at high pressures the P excitons still form a hydrogenlike series with a linear pressure dependence both of the band-gap and of the exciton Rydberg. This pressure dependence was determined by a fit to the experimental data; the results are found in Table II. In Fig. 6 one can see the excellent agreement between the experimental data and this fit.

Mainly because of interaction with even-parity excitons of the green series, the energies of the even-parity excitons[4] of the yellow series (e.g., the $1S$) are different from what one would expect using the hydrogenlike series formula. Therefore, the pressure dependences of the $1S$ orthoexciton and the $1S$ paraexciton were fitted separately. As one can see from Table II, the blue shift under pressure is the same for the orthoexciton and the paraexciton. Thus the electron-hole exchange energy, which is the energy difference between orthoexciton and paraexciton, is independent of pressure. Further, the pressure shift of the $1S$ excitons is about the same as that expected by applying the hydrogenlike series formula for $n=1$ (15.0 versus 14.9 meV). This means that the interaction with excitons of the green series stays about the same. Thus one can expect for the green series a similar pressure shift as for the yellow series.

TABLE II. Exciton energies at ambient pressure and their pressure derivatives. Also included are the band-gap energy and the exciton Rydberg. All data are for $T=6$ K.

Exciton	Zero-pressure energy (eV)	Pressure derivative (meV/GPa)
$1S$ para	2.0208	15.0±0.2
$1S$ ortho	2.0327	15.0±0.1
$2P$	2.1474	13.1
$3P$	2.1611	12.8
$4P$	2.1658	12.7
$5P$	2.1681	12.6
Band gap	2.1720	12.5±0.3
Rydberg	0.0985	−2.4±0.3

Comparison of the pressure coefficients measured in this work with those reported by Laisaar *et al.*[7] shows near agreement for the pressure shifts of the band gap and of the $1S$ exciton, but a large difference for the pressure dependence of the exciton Rydberg (−2.4 versus −9.9 meV/GPa). One would not expect that the different temperatures used (6 versus 77 K) are the reason for this difference. On the other hand, the present measurements cover a much wider pressure range and are therefore expected to yield more accurate pressure coefficients.

The exciton Rydberg R in a crystal depends on the reduced mass μ of electron and hole and on the relative dielectric constant ϵ at zero frequency:

$$R=R_{\mathrm{H}}\frac{\mu}{m_0}\frac{1}{\epsilon^2}\ , \tag{3}$$

with $R_{\mathrm{H}}=13.6$ eV the Rydberg energy of hydrogen and m_0 the free electron mass. Thus the pressure dependence of the excitonic Rydberg energy may be caused by a change with pressure in the reduced exciton mass μ and the zero-frequency dielectric constant ϵ. The pressure dependence of these parameters has not been measured. One can estimate the change in ϵ by using the Lyddane-Sachs-Teller relation for phonon F (this phonon has a much larger oscillator strength[27] than the other infrared-active phonon C) and the experimental pressure coefficient of the refractive index in the red spectral range[7] $dn/dP=1.1\times10^{-2}$ GPa^{-1}. In this way a value of $d\epsilon/dP=1.5\times10^{-2}$ GPa^{-1} is obtained, which would result in a pressure coefficient of the exciton Rydberg $dR/dP=-0.42$ meV GPa^{-1}. This is much smaller than

the observed value of $dR/dP = -2.4$ meV GPa^{-1}. Thus the decrease of the exciton Rydberg with pressure appears to be mainly due to a decrease of the reduced exciton mass. One should be careful, however, because one has to rely on the value for dn/dP given in Ref. 7, which the authors themselves state as being preliminary.

Using the pressure shift of the band-gap energy and the bulk modulus given above, the gap deformation potential E_d is determined as

$$E_d = \frac{dE_g}{d\ln(V)} = -\frac{dE_g}{dP}B = -1.38 \pm 0.03 \text{ eV} .$$

From the analysis of measurements under uniaxial stress Trebin *et al.*[28] found a hydrostatic band-gap deformation potential of -2.1 eV. Compared to our case the analysis of uniaxial stress experiments is more complicated. Further, the measurements were limited to a maximum uniaxial stress of 0.3 GPa, i.e., a hydrostatic component of 0.1 GPa, so that we believe our value for the deformation potential to be the more reliable one.

IV. RIGID-ION MODEL FOR THE PHONON FREQUENCIES

We present a simple rigid-ion model which explains the rather differing values for the Grüneisen parameters of the various phonons. It is an extension of a model used by Huang,[11] Carabatos,[29] and Carabatos and Prevot.[30] Included are the Coulomb interaction between oxygen and copper ions and central and bond-bending forces between nearest neighbors. In addition, we have included central forces between second neighbors. Thus five parameters enter into this model: q, the effective charge of the Cu ions (the charge of the O ions is $-2q$); α and β, the diagonal and nondiagonal elements of the force constant tensor (axes parallel to the crystal axes) for nearest neighbors (since the O—Cu bonds are in [111] directions, the force constant for bond stretching is $\alpha+2\beta$ and for bond bending $\alpha-\beta$); γ, the force constant for the Cu-Cu interaction; δ, the force constant for the O-O interaction. After diagonalization of the dynamical matrix one finds the phonon frequencies in terms of the parameters used, as given in the Appendix.

At zero pressure the following values for the parameters are found from a fit of the calculated phonon frequencies to the experimental values: $\alpha = 75.1$ N m^{-1}, $\beta = 66.4$ N m^{-1}, $\alpha+2\beta = 207.9$ N m^{-1} (bond stretching), $\alpha-\beta = 8.7$ N m^{-1} (bond bending), $\gamma = 6.6$ N m^{-1}, $\delta = -25.3$ N m^{-1}, and $q = 0.29e$, e being the elementary charge. In the earlier work by Huang[11] and Carabatos[29] similar values for α, β, and q were determined, but no values for γ and δ, the second-neighbor force constants. The values for γ and δ obtained here signify a small attractive force between two copper atoms and a fairly strong repulsive interaction between two oxygen atoms.

For describing the pressure dependence it is assumed that the force constants α, γ, and δ vary with the inverse sixth power of the interatomic distances which would result in mode Grüneisen parameters of unity. Further, it is assumed that the effective charge stays constant with pressure. The only free parameter then is the nondiagonal force constant β. Its pressure dependence was determined from a fit to the experimental values to be $d\beta/dP = 2.15$ N m^{-1} GPa^{-1}, which corresponds roughly to an inverse tenth power dependence on interatomic distances.

The pressure dependences of phonon frequencies calculated within this model are shown in Fig. 5, together with the experimental results. The agreement is quite satisfactory, except for phonon B, where this model predicts a negative Grüneisen parameter, whereas a positive (though rather small) value is found in the experiment. Nevertheless, this model explains the pronounced difference in the pressure dependence between the low-energy (A,B,C) and the high-energy (D,E,F,F') phonons. This difference is mainly due to the different behavior of the bond-bending and bond-stretching forces with pressure. Whereas the bond-stretching force constant $\alpha+2\beta$ increases with 3.51 N m^{-1} GPa^{-1}, the bond-bending force constant $\alpha-\beta$ decreases with -0.79 N m^{-1} GPa^{-1}. In a first approximation, one would expect that a structural phase transition occurs at the pressure where this bond-bending force becomes zero. This is the case for a pressure of 11.0 GPa at a temperature of 6 K. The observed pressures for the phase transition from the cubic to the hexagonal phase[8] are ~ 10 GPa at room temperature and ~ 11 GPa at 100 K. Thus our simple model also predicts the correct pressure for the phase transition.

V. CONCLUSIONS

Using cryogenic diamond-window-cell techniques in combination with condensed helium as a pressure-transmitting medium, we have measured the pressure dependence of the low-temperature exciton luminescence in Cu_2O under nearly perfect hydrostatic conditions up to ~ 7 GPa. We find that (i) the band gap increases at a small rate of 12.5 ± 0.3 meV/GPa, which is equivalent to a band-gap deformation potential of -1.38 ± 0.03 eV; (ii) the exciton Rydberg energy decreases with -2.4 ± 0.3 meV/GPa, which we attribute mainly to a decrease of the reduced exciton mass; and (iii) the energies of both $1S$ orthoexciton and $1S$ paraexciton increase at the same rate at 15.0 meV/GPa, so that in view of our small experimental uncertainty the electron-hole exchange energy is essentially independent of pressure.

Using a combination of luminescence and Raman spectroscopy we have measured the frequencies of all six zone-center phonons in Cu_2O as a function of hydrostatic pressure at 6 K. The mode Grüneisen parameters of the zone-center phonons vary between -3.4 and $+1.7$. This wide range of Grüneisen parameters is satisfactorily explained by a rigid-ion model, which also predicts the pressure for a structural phase transition, in excellent agreement with experimental observation.

ACKNOWLEDGMENTS

We would like to acknowledge the aid of W. Böhringer and W. Dieterich in performing the experiments.

APPENDIX

The expressions for the phonon frequencies obtained from a diagonalization of the dynamical matrix are (in

terms of the five parameters α, β, γ, δ, and q, see Sec. IV) the following:

Phonon A: $\omega^2=2m_2^{-1}(1.345Q+\alpha-\beta)$;
Phonon B: $\omega^2=2m_2^{-1}(2.38Q+\alpha-\beta+\gamma)$;
Phonons C,C': $\omega^2=R+T-[(R-T)^2+S]^{1/2}$;
Phonon D: $\omega^2=2m_2^{-1}(-2.691Q+\alpha+2\beta+4\gamma)$;
Phonon E: $\omega^2=2m_1^{-1}(2\alpha+\delta)$;
Phonons F,F': $\omega^2=R+T+[(R-T)^2+S]^{1/2}$;
with $Q=q^2/\epsilon_0 a^3$;

$R=2m_3^{-1}(1.333Q+\alpha)$ for the longitudinal phonons (C,F);
$R=2m_3^{-1}(-0.667Q+\alpha)$ for the transverse phonons (C',F');
$S=16m_2^{-1}m_3^{-1}(1.69Q-\beta)^2$;
$T=m_2^{-1}(-2.035Q+\alpha+\beta+2\gamma)$;
m_1, the mass of an oxygen atom;
m_2, the mass of a copper atom;
$m_3=2m_1m_2/(m_1+2m_2)$.

[1]M. Hayashi and K. Katsuki, J. Phys. Soc. Jpn. **5**, 380 (1950).
[2]V. T. Agekyan, Phys. Status Solidi B **43**, 11 (1977).
[3]*Functional Relationships in Science and Technology,* Vol. III/17e of Landolt-Börnstein, New Series, edited by O. Madelung (Springer, Berlin, 1983).
[4]Ch. Uihlein, D. Fröhlich, and R. Kenklies, Phys. Rev. B **23**, 2731 (1981).
[5]D. Snoke, J. P. Wolfe, and A. Mysyrowicz, Phys. Rev. Lett. **59**, 827 (1987).
[6]F. I. Kreingol'd, K. F. Lider, and V. F. Sapega, Fiz. Tverd. Tela **19**, 3158 (1977) [Sov. Phys.—Solid State **19**, 1849 (1977)].
[7]A. Laisaar, A. Niilisk, F. Kreingol'd, and K. Lider, in *High Pressure in Science and Technology,* edited by B. Vodar and Ph. Marteau (Pergamon, Oxford, 1980), Vol. 2, p. 756.
[8]A. Werner and H. D. Hochheimer, Phys. Rev. B **25**, 5929 (1982).
[9]R. J. Elliott, Phys. Rev. **124**, 340 (1961).
[10]In this paper we use the notation of G. F. Koster, J. O. Dimmock, R. G. Wheeler, and H. Statz, *Properties of the Thirty-two Point Groups* (M.I.T. Press, Cambridge, MA, 1963).
[11]K. Huang, Z. Phys. **171**, 213 (1963).
[12]Elliott (Ref. 9) and Dawson, Hargreave, and Wilkinson (Ref. 27) give incorrect normal modes for phonon C.
[13]M. A. Washington *et al.*, Phys. Rev. B **15**, 2145 (1977).
[14]E. F. Gross, Usp. Fiz. Nauk **76**, 433 (1962) [Sov. Phys.—Usp. **5**, 195 (1962)].
[15]P. W. Baumeister, Phys. Rev. **121**, 359 (1961).
[16]Y. Petroff, P. Y. Yu, and Y. R. Shen, Phys. Rev. B **12**, 2488 (1975).
[17]S. Nikitine, in *Optical Properties of Solids,* edited by S. Nudelman and S. S. Mitra (Plenum, New York, 1969), p. 197.
[18]G. Huber, K. Syassen, and W. B. Holzapfel, Phys. Rev. B **15**, 5123 (1977).
[19]R. A. Forman, G. J. Piermarini, J. D. Barnett, and S. Block, Science **176**, 284 (1972); D. M. Adams, R. Appleby, and S. K. Sharma, J. Phys. E **9**, 1140 (1976).
[20]H. K. Mao, P. M. Bell, J. W. Shaner, and D. J. Steinberg, J. Appl. Phys. **49**, 3276 (1978).
[21]K. Reimann, W. Dietrich, and K. Syassen (unpublished).
[22]A. Compaan and H. Z. Cummins, Phys. Rev. B **6**, 4753 (1972).
[23]K. Reimann, J. Lumin. **40&41**, 475 (1988).
[24]A. Mysyrowicz, D. P. Trauernicht, J. P. Wolfe, and H.-R. Trebin, Phys. Rev. B **27**, 2562 (1983).
[25]J. Hallberg and R. C. Hanson, Phys. Status Solidi **42**, 305 (1970).
[26]M. Kalliomäki, V. Meisalo, and A. Laisaar, Phys. Status Solidi A **56**, K127 (1979).
[27]P. Dawson, M. M. Hargreave, and G. R. Wilkinson, J. Phys. Chem. Solids **34**, 2201 (1973).
[28]H.-R. Trebin, H. Z. Cummins, and J. L. Birman, Phys. Rev. B **23**, 597 (1981).
[29]C. Carabatos, Phys. Status Solidi **37**, 773 (1970).
[30]C. Carabatos and B. Prevot, Phys. Status Solidi B **44**, 701 (1971).